Available online at www.sciencedirect.com
ScienceDirect
Trans. Nonferrous Met. Soc. China 26(2016) 1512−1521
Transactions of Nonferrous Metals Society of China
www.tnmsc.cn

Corrosion influence on surface appearance and microstructure of compo cast ZA27/SiC_p composites in sodium chloride solution

Biljana BOBIĆ[1], Jelena BAJAT[2], Ilija BOBIĆ[3], Bore JEGDIĆ[1]

1. Institute of Chemistry, Technology and Metallurgy, University of Belgrade, Belgrade 11000, Serbia;
2. Faculty of Technology and Metallurgy, University of Belgrade, Belgrade 11000, Serbia;
3. "Vinča" Institute of Nuclear Sciences, University of Belgrade, Belgrade 11000, Serbia

Received 22 July 2015; accepted 15 March 2016

Abstract: The influence of corrosion on the surface appearance and microstructure of particulate ZA27/SiCp composites was examined after 30 d immersion in a sodium chloride solution with the access of atmospheric oxygen. The composites with different contents of SiC micro-particles were synthesized via compo casting. Microstructural studies by means of optical microscopy (OM) and scanning electron microscopy (SEM) showed that corrosion occurred in the composite matrices, preferentially in regions of the η phase, rich in zinc. The corrosion processes did not affect the silicon carbide particles incorporated in the matrix alloy. According to the results of electrochemical polarization measurements, an increase in the content of SiC particles in the composite matrice has led to the lower corrosion resistance in the composites.

Key words: metal-matrix composites; ZA27 alloy; corrosion; microstructure; polarization resistance; corrosion rate

1 Introduction

Discontinuously reinforced metal matrix composites (DRMMCs) have been developed intensively over the past several decades, because of their superior physical, mechanical, electrical and tribological characteristics relative to monolithic metal matrices. The composites have been used in many structural and industrial applications that require light weight, high strength, specific thermal properties, wear resistance. The most common commercial DRMMCs are based on aluminum, magnesium and titanium alloys whereas much less attention has been given for development of composites with a base of zinc alloys. Ceramic particles such as particles of silicon carbide (SiC), alumina (Al_2O_3), boron carbide (B_4C), titanium carbide (TiC) or graphite particles have been mainly used as reinforcements for DRMMCs. With addition of hard ceramic particles, the composite hardness increases, which has a positive effect on the wear resistance of the composites [1−3].

Zinc–aluminum (ZA) casting alloys have been widely used for different applications. The alloys are characterized by a favorable combination of physical, mechanical and technological properties (low melting point, high strength and hardness, exceptional castability, easy machining, good corrosion resistance in atmospheric conditions) and low manufacturing costs. ZA alloys are also important bearing materials. Amongst the family of ZA alloys, the alloy with 27% aluminum (ZA27 alloy) is distinguished by the highest tensile strength and excellent wear resistance properties. The alloy has been used in sliding bearings and bushing applications, particularly for high-load and low-speed conditions [4]. However, at temperatures above 100 °C, a deterioration of the alloy properties was observed. To overcome this disadvantage, different thermally stable ceramic particles have been incorporated in the ZA27 alloy and the composites with the base of this alloy have been produced [5−9]. It was noticed that the presence of glass fibres [6] or hard particles of garnet [5], zircon [10] and SiC [7,8,11] in the ZA27 alloy led to a significant improvement in hardness and wear resistance of the composites relative to the matrix alloy.

The ZA27 alloy solidifies in a wide temperature range and is suitable for processing in the semi-solid state. MMCs with the ZA27 alloy matrices have been most commonly synthesized using the stir casting or compo casting technique. The compo casting technique involves intensively mixing of a semi-solid matrix alloy

Corresponding author: Biljana BOBIĆ; E-mail: biljanabobic@gmail.com
DOI: 10.1016/S1003-6326(16)64257-7

and a composite mixture, so that the primary phase becomes non-dendritic, giving thus a composite mixture with thixotropic properties [12−16].

Application of MMCs in various environments (atmospheric conditions, natural waters, water solutions etc.) requires the adequate corrosion resistance of the composites. The presence of discontinuous reinforcements and methods of producing MMCs can cause accelerated corrosion of the metal matrices relative to corrosion of monolithic matrix alloys [17]. Corrosion resistance of DRMMCs depends on the chemical composition of the matrix alloy and reinforcements, on the reinforcement shape, size, content and distribution in the metal matrix and also at the interface between the matrix and reinforcements. The presence of particulate reinforcements may influence the composite microstructure by inducing dislocation generation, formation of intermetallic compounds, the appearance of micro-cracks in the composite matrix [12] and crevice corrosion at the matrix/particle interface [1]. All this can significantly affect corrosion resistance of the MMCs.

There have been few studies on the corrosion behavior of composites with a base of the ZA27 alloy. It was revealed in these studies that corrosion rate decreases with increase in the content of reinforcements (zircon, graphite, glass fibers) in the composites [18−20]. However, there have been no reported results on the corrosion of composites with the ZA27 alloy as the matrix and SiC micro-particles as the secondary phase.

Electrochemical techniques may be also applied to obtaining corrosion rates of the composites, if corrosion is predominantly uniform on the composite surface. The linear polarization technique and recording of Tafel graphs have been commonly used to obtain the corrosion current density J_{corr}. Recently, these electrochemical techniques were applied to determining the corrosion rate of the ZA27 alloy [21,22].

Corrosion behavior of binary ZA alloys depends on their surface composition which may change due to selective dissolution phenomena [23]. Selective dissolution of zinc was observed at the initial stage of the exposure of a ZA alloy to the marine environment, while dissolution of aluminum from the alloy was noticed at the later stage [24,25].

MMCs with the base of ZA27 alloy and SiC particles as the reinforcements are intended for different tribological applications because of the high hardness and significantly improved wear resistance relative to the matrix alloy. Microstructural and mechanical characteristics, wear resistance and aging phenomena of these composites have been the subject of various studies [7,8,11,26], whereas much less research has been devoted to their behavior in different corrosive media.

The aim of this work was to study the influence of corrosion on the surface appearance and microstructure of the ZA27/SiC_p composites during their immersion in a sodium chloride solution. An attempt was also made to determine the effect of the relative content of the SiC particles incorporated in the metal matrix on the corrosion resistance of these composites.

2 Experimental

2.1 Materials

The commercially available ZA27 alloy was used as the composite matrix. The chemical composition of the alloy is given in Table 1.

Table 1 Chemical composition of ZA27 alloy (mass fraciton, %)

Al	Cu	Mg	Zn
26.3	1.54	0.018	Bal.

The ZA27 alloy was conventionally melted and cast. SiC particles with the average particle size of 40 μm were used as the reinforcement for the ZA27 alloy. The composites with 1%, 3% or 5% SiC particles were synthesized via compo casting using a suitable experimental equipment [27]. The matrix alloy was superheated above its melting temperature. The alloy melt was then cooled down to the operating temperature (465 °C) using the cooling rate of 5 K/min, when a homogenizing mixing (450 r/min) was applied for 10 min. After homogenization, SiC particles (preheated at 450 °C to remove the moisture) were added in the semi-solid melt of the matrix alloy, with simultaneous slow mechanical mixing (450 r/min). The addition was carried out at 465, 470 or 475 °C, for 3, 5 or 7 min, respectively, depending on the planned content of SiC particles in the ZA27/SiC_p composites. After the addition of particulate reinforcements, the mixing speed was increased to 1000 r/min (with isothermal mixing for 2.5 min), and then to 1500 r/min (with isothermal mixing of the composite mixture for 7.5 min). The composite mixture was cooled down to 460 °C with the cooling rate of 5 K/min and then poured into a steel mold preheated at 300 °C. Castings (20 mm × 30 mm × 120 mm) of the ZA27/SiC_p composites with different contents of SiC particles were cut to obtain composite samples (20 mm × 30 mm × 5.5 mm) for hot pressing. The samples were hot pressed at 350 °C, under the pressure of 250 MPa. Specimens for hardness measurements, microstructural examinations and electrochemical polarization measurements were cut from the hot pressed samples. Composite specimens with 1%, 3% or 5% SiC particles will be marked further as the C1, C2 and C3 composite, respectively.

2.2 Methods

2.2.1 Hardness measurements

Hardness measurements were conducted in accordance with ASTM E10 [28]. The hardness test was performed at room temperature on plate-like specimens (15 mm × 15 mm × 6 mm) using a Brinell hardness tester, with a ball indenter of 2.5 mm in diameter and a load of 62.5 kg. The load was applied for 30 s. Three specimens of each composite type were tested. At least five hardness readings were taken for each specimen at different locations and the average hardness value was calculated.

2.2.2 Microstructural examinations

Surface appearance and microstructure of the ZA27/SiC_p composites were examined by means of optical microscopy (OM) and scanning electron microscopy (SEM) with energy-dispersive X-ray spectroscopy (EDS) using an optical microscope (Carl Zeiss) and a JEOL JSM 5800LV scanning electron microscope coupled with an Oxford Link ISIS energy dispersive X-ray spectrometer. Composite specimens (5 mm in diameter and 8 mm in height) were prepared by grinding and polishing. Wet grinding was carried out with progressively finer abrasive SiC papers (240, 360, 600 and 800 grits) while polishing was done using a polishing cloth and the diamond polishing paste (2 μm in particle size). Polished specimens were used for SEM/EDS analysis, whereas specimens for OM studies were polished or etched in a water solution of nitric acid (9% HNO_3, volume fraction).

Composite specimens were examined before and after the immersion test. Constant immersion of the specimens was performed in the stagnant solution of the sodium chloride (3.5% NaCl, pH 6.7) at room temperature and lasted for 30 d. The solution was open to the atmospheric air. Before the test all specimens were cleaned with acetone and dried in the air.

2.2.3 Electrochemical polarization measurements

Corrosion rates of the ZA27/SiC_p composites were determined by means of the linear polarization technique and from recorded Tafel graphs. Electrochemical polarization measurements were performed in a three-electrode electrochemical cell, using a Gamry Reference 600 Potentiostat. The cell is intended for flat specimens, with 1 cm^2 contact area between the working electrode and the test solution. A saturated calomel electrode (SCE) was used as the reference electrode and a platinum mesh as the counter electrode. The measurements were carried out in the the unstirred test solution open to atmosphere, at room temperature. The composite specimens (30 mm × 20 mm × 3 mm) of each composite type (C1, C2 and C3) were used as working electrodes. Before electrochemical tests, each specimen was wet ground using progressively finer abrasive SiC papers (down to 800 grits), rinsed with distilled water and acetone and then air-dried. After that it was immediately transferred to the electrochemical cell with the test solution (3.5% NaCl, pH 6.7). The working electrode was kept in the test electrolyte about 30 min to 60 min to establish the relatively stable open-circuit potential (φ_{OCP}) and then it was polarized to −15 mV (relative to the φ_{OCP}), at a scan rate of 0.2 mV/s. The potential scan was applied over the 30 mV range (from the cathodic towards the anodic side) with the same scan rate. The polarization resistance R_p was determined from the slope of the recorded $\varphi-J$ graphs, at the φ_{OCP}.

After each linear polarization test, the working electrode was allowed to return spontaneously to the φ_{OCP}. The electrode was then polarized to ±0.250 V (relative to the φ_{OCP}), starting from the cathodic side, with a scan rate of 0.2 mV/s. The resulting current was plotted against potential on a logarithmic scale. The J_{corr} and Tafel slopes b_a and b_c were determined from the recorded $\varphi-\lg J$ graphs.

3 Results and discussion

3.1 Hardness

The measured hardness values for the C1, C2 and C3 composite are shown in Table 2.

Table 2 Hardness of ZA27/SiC_p composites

Composite	Hardness (HB)	Standard deviation
C1	132	3.7
C2	137	4.8
C3	116	8.5

The hardnesses of the composites C1 and C2 are higher than that of the as-cast ZA27 alloy [29] while the hardness of the composite C3 is slightly lower. The increase in the content of particulate reinforcements from 1% to 3% in the ZA27/SiC_p composites, resulted in the increase in hardness values, in accordance with Ref. [7]. This could be explained by strengthening of the composite matrices due to the presence of hard SiC particles in the composites C1 and C2 [30]. A higher content of SiC particles in the C3 composite (5%) resulted in a lower hardness of this composite when compared with the hardness of the composites C1 and C2. This could be related with the presence of agglomerates of SiC particles in the composite C3.

3.2 Surface appearance and microstructure

Composite specimens were immersed in the test solution for 30 d. Changes in the surface morphology and microstructure of the specimens were noticed after

this time, because of the occurrence of corrosion process in the composite matrices during the immersion. Representative micrographs of the composite specimens before and after the immersion test, obtained by means of OM and SEM, are presented in Figs. 1−6.

The surface appearance of composite specimens with different contents of SiC particles is shown in Fig. 1. SiC particles are clearly visible in the composite matrices. Distribution of the particles is mainly uniform in the composites C1 and C2, with minimal agglomeration (Figs. 1(a) and (b)). In these composites, the matrix/particle interface is continuous in most cases, while contact between SiC particles is rare.

Agglomerates and clusters of SiC particles can be noticed in the composite C3 (Figs. 1(c) and (d)). The matrix/particle interface is not continuous in the clusters, which results in a weak bond between SiC particles. However, cavities which may arise due to the fallout of SiC particles from the composite matrices (for example during metallographic preparation of the composite specimens) are not visible, which indicates good bonding between the composite matrix and particulate reinforcements. Several micro-cracks near the matrix/particle interface can be noticed in the composites C2 and C3 (Figs. 1(b)−(d)). Initial micro-cracks were probably formed during solidification of the composite mixtures after the compo casting process, due to the different linear coefficients of thermal expansion of the ZA27 alloy ($26\times10^{-6}\ K^{-1}$) and SiC particles ($4.0\times10^{-6}\ K^{-1}$).

The microstructure of the composite matrices is morphologically similar in all ZA27/SiC_p composites. The microstructure of the composite with 5% SiC_p is shown in Fig. 2. The specific microstructure of the composite matrix was formed during the compo casting process. It is well known that the microstructure of the matrix alloy (the as-cast ZA27 alloy) consists of a dendritic phase, rich in aluminum, and interdendritic regions, rich in zinc [31,32]. In the process of compo casting, dendritic structure of the matrix alloy has been transformed under the influence of shear forces caused by the mechanical mixing of the semi-solid mixture. The transformation was carried out in accordance with Fleming's scheme [33] so that primary particles of the α phase became elliptical and globular. The primary particles are clearly visible in the composite matrix (Fig. 2). They consist of a core (the α phase, rich in aluminum) and a periphery (the phase mixture $\alpha+\eta$). The η phase, rich in zinc, is placed between the primary particles. It was shown recently that different phases in the microstructure of ZA alloys contributed differently to the corrosion resistance of these alloys [23]. SiC particles in the composite C3 are mainly distributed in the regions of the η phase and partly in the regions of the $\alpha+\eta$ phase mixture.

One SiC particle, incorporated into the metal matrix of the composite C3, is clearly visible at higher magnifications (Figs. 3(a) and (b)). The particle is mainly surrounded with the phase mixture $\alpha+\eta$. The surface of the particle is smooth and clean, without products of chemical reactions at the matrix/particle interface. This suggests a mechanical bond between the metal matrix and the particle. The addition of SiC particles in the semi-solid melt of the matrix alloy (during compo casting) was carried out at a relatively

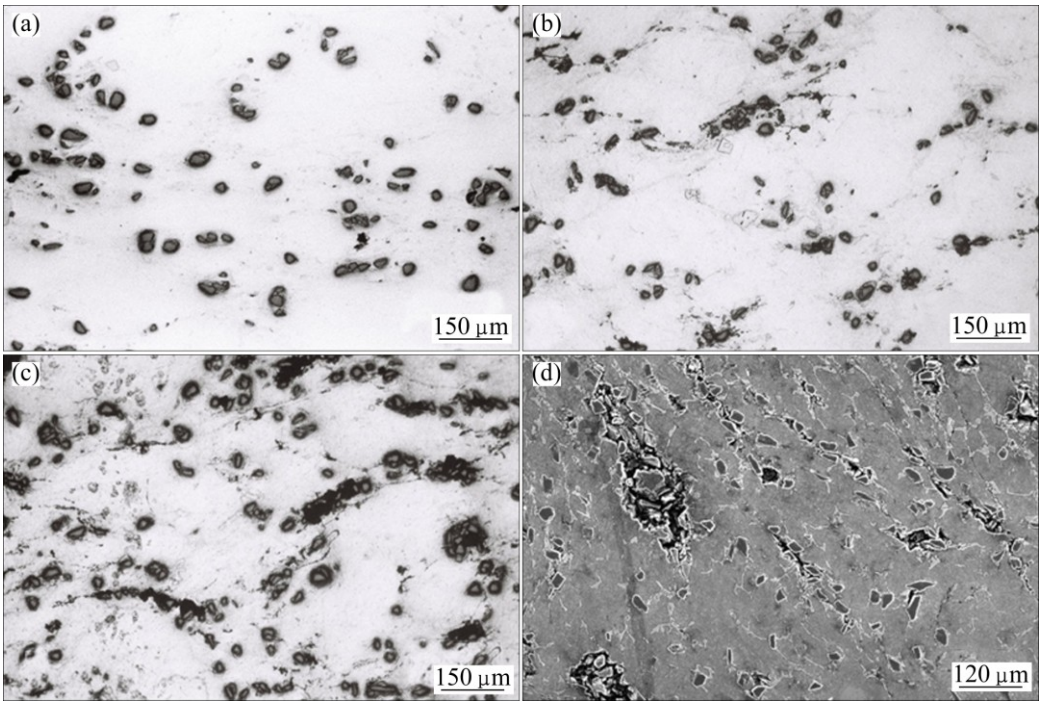

Fig. 1 Surface appearance of ZA27/SiC_p composites before immersion test, OM, polished: (a) C1; (b) C2; (c) C3; (d) C3, SEM/SE

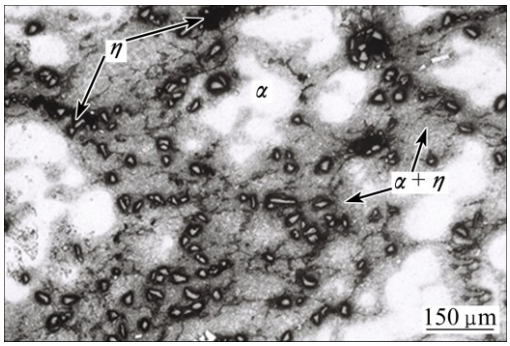

Fig. 2 Microstructure of composite C3 before immersion test, OM, etched

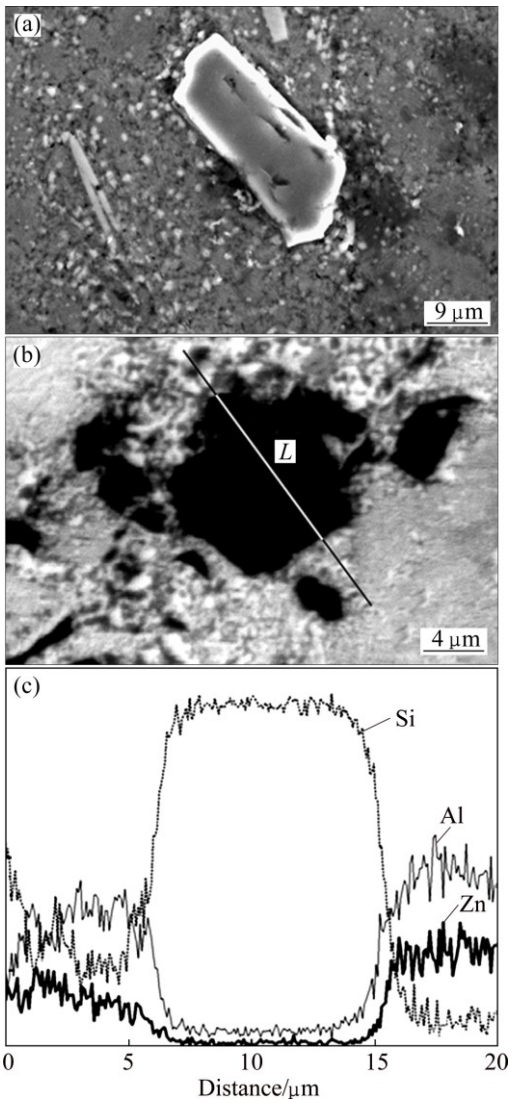

Fig. 3 Microstructure of composite C3 before immersion test: (a, b) One SiC particle incorporated in composite matrix (detail) SEM/SE; (c) Changes in chemical composition in region around SiC particle, SEM/EDS

low temperature, so that there were no chemical reactions between the alloy melt and the particles.

In this work, the composites were synthesized without a formation of chemical compounds at the operating temperature of the applied compo casting process.

Changes in the chemical composition of the composite matrix in the region around the SiC particle are presented in Fig. 3(c). The position of the line analysis is shown in Fig. 3(b).

The concentration of silicon reaches maximum in the region of the particle, confirming the presence of SiC particles in the composite matrix. Concentrations of aluminum and zinc are consistent with their contents in the phase mixture $\alpha+\eta$ (Fig. 3(c)). The presence of chemical compounds at the matrix/particle interface was not detected by means of the SEM/EDS analysis, which is in accordance with observations in Fig. 3(a).

Before the immersion in the test solution, the surface of the ZA27/SiC_p composites was covered with an oxide layer. The zinc-rich regions in the composite matrices were covered with a zinc oxide film while the oxide film on the aluminum-rich phase was an aluminum oxide or a mixed zinc−aluminum oxide [25,34]. Surface morphology and microstructure of the composites were changed during the immersion in the test solution because of the occurrence of corrosion processes in the composite matrices. Surface appearance of all composite specimens (with different contents of SiC particles) was found to be similar after the immersion test. The surface appearance of the composite C3 specimen before and after the immersion test is shown in Fig. 4. It can be seen that the corrosion attack begins from the edge of the specimen and spreads over its surface. As it was expected, the corrosion processes did not influence SiC particles incorporated in the composite matrix, due to the inherent chemical stability of the particles. This is clearly visible in Figs. 4(b) and (c).

The presence of micro-cracks was noticed close to the SiC particles in all composite matrices, whereas micro-cavities were mainly found in the composite C3, in places where clusters of SiC particles were formed. Micro-cavities and micro-cracks are clearly visible on the surface of the composite C3 specimen (Fig. 4(b)). During the immersion test, corrosion processes in the initial micro-cracks and micro-cavities led to an increase in their size.

The microstructure of the C3 composite after the immersion test is shown in Fig. 5. Primary particles of the α phase are clearly visible in the composite matrix, whereas SiC particles are placed mainly in the η phase of the composite (Fig. 5). Corrosion did not affect SiC particles, which is consistent with observations in Figs. 4(b) and (c).

The process of corrosion occurred preferentially in the η phase and in the region of the $\alpha+\eta$ phase mixture.

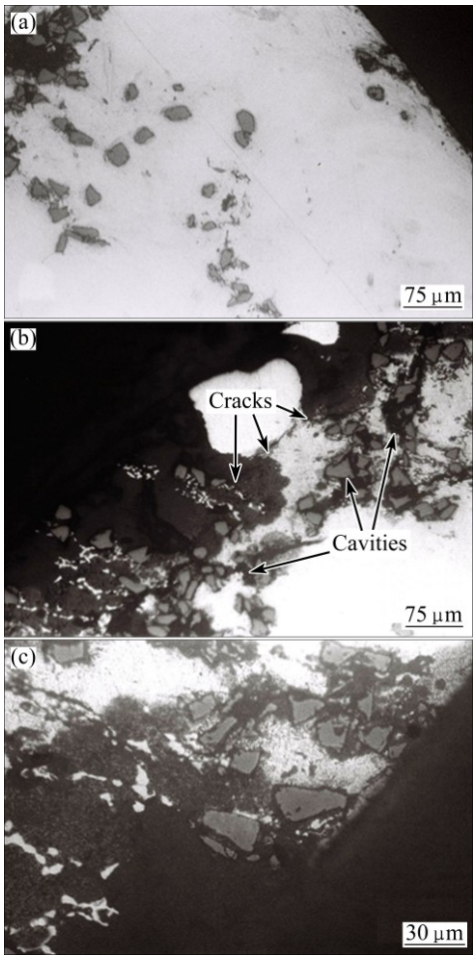

Fig. 4 Surface appearance of composite C3, OM, polished: (a) Before immersion test; (b, c) After immersion test

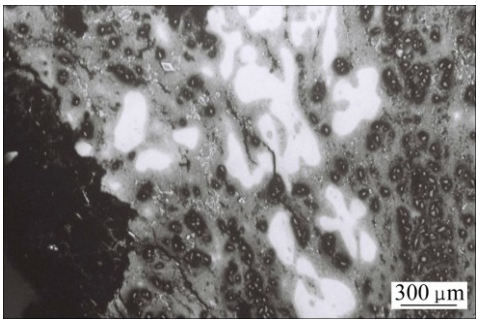

Fig. 5 Microstructure of composite C3 after immersion test, OM, etched

As can be seen, dissolution of the composite matrix is mainly uniform. The regions rich in zinc are susceptible to the corrosion attack, while the aluminum-rich areas are much more resistant. This is consistent with earlier observations [24,25].

Surface morphology of the composite specimens after the immersion test was examined by means of SEM. Typical images presented in Fig. 6 reveal that the composite surface is covered with a layer of corrosion products. The porous layer consisting of white and crumbly corrosion products was formed during the immersion in the sodium chloride solution.

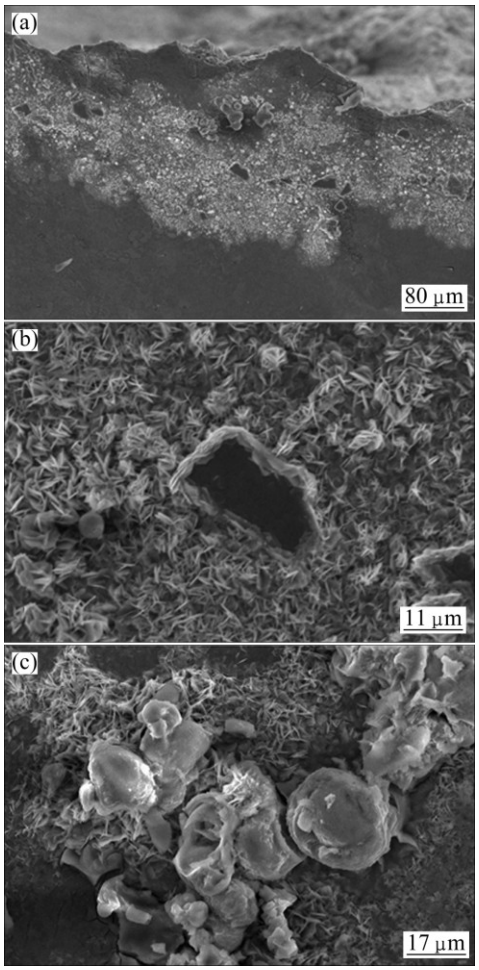

Fig. 6 Surface morphology of composite C1 after immersion test, SEM/SE: (a) Surface appearance; (b) One SiC particle surrounded with corrosion products (detail); (c) Morphology of corrosion products

Corrosion did not influence SiC particles in the composite matrix (Figs. 6(a) and (b)), which is in accordance with other results of microstructural studies (Figs. 4(b) and (c) and Fig. 5). The particles are surrounded with corrosion products (Fig. 6(b)). The corrosion products are mainly needle-shaped and rosette-like (Fig. 6(c)). They were formed during the occurrence of corrosion processes in the composite matrix. $Zn(OH)_2$ and ZnO were shown to be the main corrosion products after the constant immersion of the ZA27 alloy in the unstirred solution of sodium chloride [21]. The presence of ZnO and $Zn(OH)_2$ was also detected in X-ray diffraction (XRD) patterns for zinc after the immersion in a sodium chloride solution [35].

3.3 Polarization resistance and corrosion rate

According to the results presented above, SiC

particles incorporated in the matrix alloy were completely resistant to the corrosion attack during the immersion test. A relatively uniform dissolution of the zinc-rich regions (the η phase and the $\alpha+\eta$ phase mixture) in the composite matrices was observed due to the occurence of corrosion processes.

Corrosion rates of the composites were determined using the linear polarization technique and Tafel graphs. First technique involves recording of the potential–current (φ–J) curve in the vicinity of the φ_{OCP}. The R_p value is determined from the slope of the linear region in this curve. The corrosion current density J_{corr} is directly related to R_p.

Experimental graphs obtained using the linear polarization technique are shown in Figs. 7(a)−(c).

Values of R_p were determined from the recorded graphs, for each composite material. The highest R_p value (1550 $\Omega\cdot cm^2$) was obtained in the case of the composite C1, while the lowest R_p value was obtained for the composite C3 (1220 $\Omega\cdot cm^2$). A small decrease in the R_p value can be noticed with increasing the content of SiC particles in the ZA27/SiC_p composites from 1% to 5%.

Experimental R_p values were introduced in the Stern–Geary equation, in order to calculate the corrosion current density J_{corr}:

$$J_{corr}=\frac{b_a b_c}{2.3(b_a+b_c)R_p} \quad (1)$$

where b_a and b_c refer to the anodic and cathodic Tafel slopes, respectively.

This equation is valid where both the anodic and cathodic polarization curves are under activation control. If the cathodic process is controlled by diffusion, the cathodic Tafel slope b_c can be taken to be infinity for the region where a limiting diffusion current density is observed. Thus, with $b_c \to \infty$, Eq. (1) reduces to

$$J_{corr}=\frac{b_a}{2.3R_p} \quad (2)$$

Equation (2) is applicable for the system in which the cathodic reaction is under diffusion control [36].

The corrosion of zinc in chloride solutions involves a charge-transfer controlled dissolution of zinc, with a formation of corrosion products on the zinc surface. When the zinc surface is free of corrosion products, the corrosion process may be controlled by a charge-transfer controlled dissolution and/or by the diffusion of a cathodic reactant. In neutral solutions open to the atmosphere, the dissolved oxygen is the main cathodic reactant [37]. Several studies on zinc corrosion in neutral media have found that the zinc corrosion process is limited by a diffusion-controlled oxygen reduction reaction [38,39].

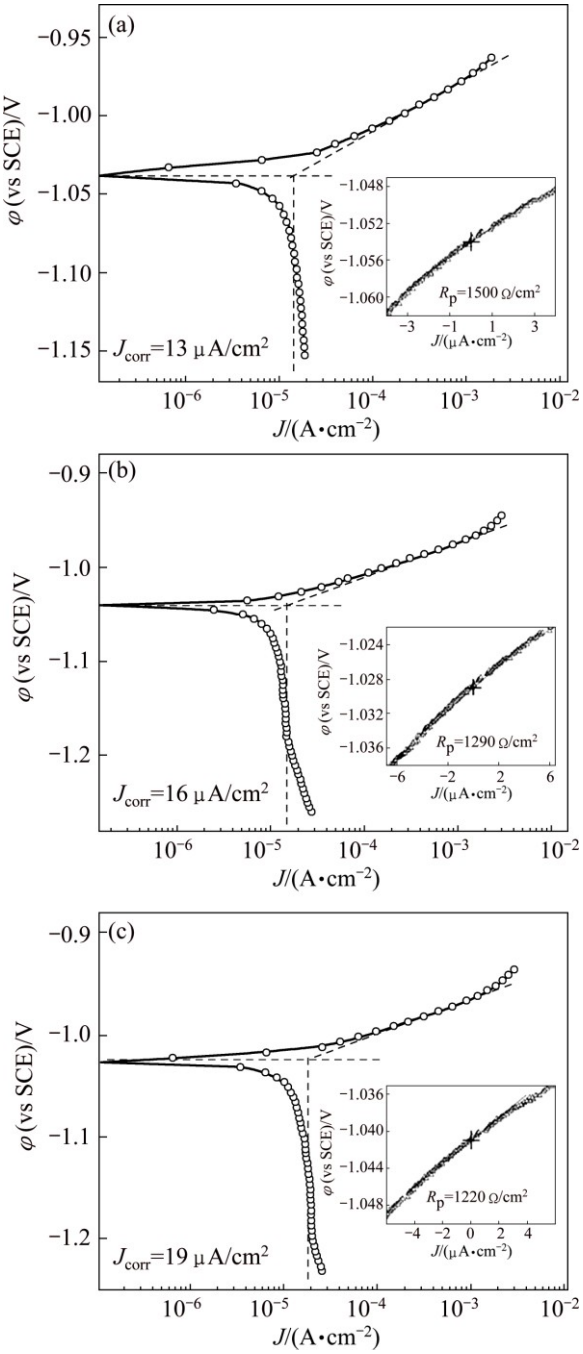

Fig. 7 Experimental Tafel graphs and polarization resistance graphs for ZA27/SiC_p composites in test solution (3.5% NaCl, pH 6.7): (a) Composite C1; (b) Composite C2; (c) Composite C3

J_{corr} values for the ZA27/SiC_p composites with different contents of particulate reinforcement were calculated using the modified Stern–Geary expression, i.e., Eq. (2). Values of b_a and b_c were obtained from experimental Tafel graphs (Figs. 7(a)−(c)). The anodic Tafel slope b_a is approximately 40 mV per decade, which is consistent with the anodic Tafel slope for dissolution of pure zinc in sodium chloride solutions [37]. The cathodic Tafel slope $b_c \to \infty$, because the cathodic reaction

is controlled by the oxygen diffusion in the test solution. The J_{corr} values, calculated using Eq. (2), are 11, 13 and 14 μA/cm^2 for the composite with 1%, 3% and 5% SiC particles, respectively. The J_{corr} values are very close and present the corrosion rate at the moment of measurement.

Similar results for the corrosion rate of the composites were obtained from the recorded Tafel graphs (Figs. 7(a)−(c)). After each linear polarization test, a corresponding Tafel graph was recorded, as described in Section 2.2.3. The graphs allow direct measurements of the corrosion current by extrapolating linear parts of the recorded dependences φ−lg J back to their intersection. The value of either the anodic or the cathodic current at the intersection is the corrosion current.

The anodic branch of the polarization curves φ−lg J (Figs. 7(a)−(c)) shows an increase in the current density with the increase in the applied polarization, indicating the anodic dissolution of the composite matrix (zinc-rich regions in the ZA27 alloy) and the activation control of the process. The value of the anodic Tafel slope b_a is between 35 and 40 mV per decade, in accordance with Ref. [37]. It was demonstrated recently that zinc dissolution from ZA alloys during linear scanning polarization was not affected by the presence of aluminum in the alloys [23]. This is consistent with observations in Section 3.2 in this work.

In the cathodic region of the polarization curves a plateau in the current density is clearly visible. This behavior is characteristic for a process controlled purely by diffusion [36]. In the test solution (3.5% NaCl, pH 6.7) open to the atmospheric air, the transport of oxygen to the electrode surface is limited due to a low solubility of oxygen in sodium chloride solutions. Accordingly, the oxygen reduction which is the major cathodic reaction in the corrosion of the ZA27/SiC$_p$ composites is completely under the mass transfer control. As can be seen in Figs. 7(a)−(c), the current becomes independent of the electrode potential for the potentials more negative than −1070 mV (vs SCE), whereas the cathodic Tafel slope $b_c \rightarrow \infty$. In that case, extrapolation of the anodic Tafel slope back to φ_{OCP} gives the value of J_{corr} which is the same as the limiting diffusion current density for the oxygen reduction [36]. In this work, the anodic Tafel slope for the zinc dissolution (in the composite matrix) was extrapolated back to φ_{OCP} and J_{corr} values for the composites C1, C2 and C3 were determined. Obtained values (13, 16 and 19 μA/cm^2 for the composites C1, C2 and C3, respectively) are in a very good agreement with the J_{corr} values obtained when using the linear polarization technique. The J_{corr} values for the ZA27/SiC$_p$ composites are somewhat higher than that for the monolithic matrix alloy in the same corrosive medium [21,22].

The results of microstructural examinations have shown that corrosion was more intensive in the composite with 5% SiC particles than that in the composites with 1% or 3% SiC particles, because of a larger number of micro-cavities and micro-cracks in the composite C3. SiC is semiconductive, so it cannot participate in cathodic reaction. The only reason of increased corrosion rate in the composite C3 is the presence of micro-cavities and micro-cracks. Corrosion processes are intensified on these active sites as mentioned above, initial micro-cracks were formed during solidification of composite mixtures due to the different linear coefficients of thermal expansion of the matrix alloy and incorporated SiC particles, whereas micro-cavities were mainly formed in the agglomerates of SiC particles. Inside micro-cavities and micro-cracks corrosion processes are of a local character. The occurrence of corrosion processes in the micro-cavities and micro-cracks during the immersion test led to an increase in their size, as shown in Section 3.2.

Results obtained in this work show that the corrosion rate of ZA27/SiCp composites increases with increasing content of SiC micro-particles in the metal matrix. These results are inconsistent with the published results [18−20]. Actually, the real comparison is not possible, because tested composites [18−20] were synthesized via different procedures, with different particles of secondary phases (zircon, graphite or short glass fibers) in the matrix ZA27 alloy. In addition, testing of corrosion resistance was performed in a solution of HCl [18−20], where the matrix alloy corrodes according to the mechanism which substantially differs from the mechanism in neutral solutions.

It can be expected that a more homogeneous distribution of SiC particles, with minimal formation of micro-cavities and micro-cracks, will result in a higher corrosion resistance of the ZA27/SiC$_p$ composites produced via compo casting. This can be achieved by specific corrections of the compo casting parameters during the composite synthesis, which is particularly important in the case of composites with a higher content of particulate reinforcements.

In summary, the results of performed micro structural examinations and electrochemical measurements indicate lower corrosion resistance of the ZA27/SiC$_p$ composites with a higher content of SiC particles. Lower corrosion resistance of the composites compared with the monolithic ZA27 alloy should be taken into account when considering the use of the ZA27/SiC$_p$ composites in marine environments.

4 Conclusions

1) Surface appearance and microstructure of the ZA27/SiC$_p$ composites have been significantly changed

after their immersion in the neutral sodium chloride solution, due to the occurrence of corrosion processes in the composite matrices.

2) Anodic dissolution of the composite matrices has occurred preferentially in the regions of the η phase which is rich in zinc and in the regions of the $\alpha+\eta$ phase mixture.

3) Corrosion did not affect SiC particles in the composite matrices.

4) In a sodium chloride solution, ZA27/SiC_p composites with a higher content of SiC particles showed lower corrosion resistance compared with the composites with a minor content of particulate reinforcements.

Acknowledgements

The Ministry of Education, Science and Technological Development of the Republic of Serbia has supported financially this work through projects TR 35021 and OI 172005. The authors are gratefully acknowledged to RAR® Foundry Ltd., Batajnica (Belgrade, Serbia) and to Ginić Tocila® Abrasive Products Factory Ltd., Barajevo (Belgrade, Serbia) for providing the master alloy and SiC particles for the research.

References

[1] ALMAN D E. Properties of metal-matrix composites in ASM handbook: Composites [M]. Vol. 21. Ohio: ASM International, 2001.

[2] SMITH C A. Discontinuous reinforcements for metal-matrix composites in ASM handbook: Composites [M]. Vol. 21. Ohio: ASM International, 2001.

[3] CHEN Fei, WANG Tong-min, CHEN Zong-ning, MAO Feng, HAN Qiang, CAO Zhi-qiang. Microstructure, mechanical properties and wear behaviour of Zn−Al−Cu−TiB_2 in situ composites [J]. Transactions of Nonferrous Metals Society of China, 2015, 25(1): 103−111.

[4] BARNHURST R J. ASM handbook, Properties and selection: Nonferrous alloys and special purpose materials [M]. Vol. 2. Ohio: ASM International, 1990.

[5] RANGANATH G, SHARMA S C, KRISHNA M. Dry sliding wear of garnet reinforced zinc/aluminium metal matrix composites [J]. Wear, 2001, 251: 1408−1413.

[6] SHARMA S C, SEAH K H W, SATISH M, GIRISH B M. Effect of short glass fibers on the mechanical properties of cast ZA27 alloy composites [J]. Materials and Design, 1996, 17: 245−250.

[7] MISHRA S K, BISWAS S, SATAPATHY A. A study on processing, characterization and erosion wear behavior of silicon carbide particle filled ZA-27 metal matrix composites [J]. Materials and Design, 2014, 55: 958−965.

[8] ABOU EL-KHAIRA M T, LOTFYA A, DAOUDA A, EL-SHEIKH A M. Microstructure, thermal behavior and mechanical properties of squeeze cast SiC, ZrO_2 or C reinforced ZA27 composites [J]. Material Science and Engineering A, 2011, 528: 2353−2362.

[9] SHARMA S C, GIRISH B M, SOMASHEKAR D R, KAMATH R, SATISH B M. Mechanical properties and fractography of zircon-particle-reinforced ZA-27 alloy composite materials [J]. Composite Science and Technology, 1999, 59: 1805−1812.

[10] SHARMA S C, GIRISH B M, SOMASHEKAR D R, SATISH B M, KAMATH R. Sliding wear behavior of zircon particles reinforced ZA-27 alloy composite materials [J]. Wear, 1999, 224: 89−94.

[11] SHARMA S C, GIRISH B M, KAMATH R, SATISH B M. Effect of SiC particle reinforcement on the unlubricated sliding wear behavior of ZA-27 alloy composites [J]. Wear, 1997, 213: 33−40.

[12] CHUNG D D L. Composite materials: Functional materials for modern technologies [M]. London: Springer-Verlag, 2003.

[13] KHOSRAVI H, BAKHSHI H, SALAHINEJAD E. Effects of compocasting process parameters on microstructural characteristics and tensile properties of A356−SiC_p composites [J]. Transactions of Nonferrous Metals Society of China, 2014, 24(8): 2482−2488.

[14] KHOSRAVI H, AKHLAGHI F. Comparison of microstructure and wear resistance of A356−SiC_p composites processed via compocasting and vibrating cooling slope [J]. Transactions of Nonferrous Metals Society of China, 2015, 25(8): 2490−2498.

[15] AMIRKHANLOU S, NIROUMAND B. Synthesis and characterization of 356-SiC_p composites by stir casting and compocasting methods [J]. Transactions of Nonferrous Metals Society of China, 2010, 20(3): 788−793.

[16] MAZAHERY A, SHABANI M O. Microstructural and abrasive wear properties of SiC reinforced aluminum-based composite produced by compocasting [J]. Transactions of Nonferrous Metals Society of China, 2013, 23(7): 1905−1914.

[17] HIHARA L H. ASM handbook: Corrosion: Materials [M]. Vol. 13B. Ohio: ASM International, 2005.

[18] SHARMA S C, SEAH K H W, SATISH B M, GIRISH B M. Corrosion characteristics of ZA-27/glass-fiber composites [J]. Corrosion Science, 1997, 39: 2143−2150.

[19] SEAH K H W, SHARMA S C, GIRISH B M. Corrosion Characteristics of ZA-27-Graphite particulate composites [J]. Corrosion Science, 1997, 39: 1−7.

[20] SHARMA S C, SOMASHEKAR D R, SATISH B M. A note on the corrosion characteristic of ZA-27/zircon particulate composites in acidic medium [J]. Journal of Materials Processing Technology, 2001, 118: 62−64.

[21] BOBIC B, BAJAT J, ACIMOVIC-PAVLOVIC Z, RAKIN M, BOBIC I. The effect of T4 heat treatment on the microstructure and corrosion behaviour of Zn27Al1.5Cu0.02Mg alloy, [J]. Corrosion Science, 2011, 53: 409−417.

[22] BOBIC B, BAJAT J, ACIMOVIC-PAVLOVIC Z, BOBIC I, JEGDIC B. Corrosion behaviour of thixoformed and heat-treated ZA27 alloys in NaCl solution [J]. Transactions of Nonferrous Metals Society of China, 2013, 23(4): 931−941.

[23] VU Thanh-nam. Selective dissolution from Zn−Al alloy coatings on steel [D]. Paris: Pierre and Marie Curie University, 2012.

[24] PALMA E, PUENTE J M, MORCILLO M. The atmospheric corrosion mechanism of 55%Al−Zn coating on steel [J]. Corrosion Science, 1998, 40: 61−68.

[25] PERSSON D, THIERRY D, LEBOZEC N. Corrosion product formation on Zn55Al coated steel upon exposure in a marine atmosphere [J]. Corrosion Science, 2011, 53: 720−726.

[26] LI Zi-quan, ZHOU Heng-zhi, LUO Xin-yi, WANG Tao, SHEN Kai. Aging microstructural characteristics of ZA27 alloy and SiCp/ZA-27 composites [J]. Transactions of Nonferrous Metals Society of China, 2006, 16(1): 98−104.

[27] AĆIMOVIĆ-PAVLOVIĆ Z, RAIĆ K T, BOBIĆ I, BOBIĆ B. Synthesis of ZrO_2 particles reinforced ZA25 alloy composites by compocasting process [J]. Advanced Composite Materials, 2011, 20: 375−384.

[28] ASTM E10-12. Standard Test Method for Brinell Hardness of Metallic Materials [S].

[29] ASTM B86-13. Standard Specification for Zinc and Zinc-Aluminum (ZA) Alloy Foundry and Die Castings [S].

[30] ARSENAULT R J, WANG L, FENG C R. Strengthening of composites due to microstructural changes in the matrix [J]. Acta Metallurgica et Materialia, 1991, 39: 47−57.

[31] MURPHY S, SAVASKAN T. Metallography of Zn−25%Al based alloys in the as-cast and aged conditions [J]. Practical Metallography, 1987, 24: 204−221.

[32] LIU Yang, LI Hong-ying, JIANG Hao-fan, LU Xiao-chao. Effects of heat treatment on microstructure and mechanical properties of ZA27 alloy [J]. Transactions of Nonferrous Metals Society of China, 2013, 23(3): 642−649.

[33] FLEMINGS M C. Behavior of metal alloys in the semisolid state [J]. Metallurgical Transactions A, 1991, 22: 957−981.

[34] ZHANG Xian, VU Thanh-nam, VOLOVITCH P, LEYGRAF C, OGLE K, WALLINDER I O. The initial release of zinc and aluminum from non-treated Galvalume and the formation of corrosion products in chloride containing media [J]. Applied Surface Science, 2012, 258: 4351−4359.

[35] MOUANGA M, RICQ L, DOUGLADE J, BERÇOT P. Corrosion behaviour of zinc deposits obtained under pulse current electrodeposition: Effects of coumarin as additive [J]. Corrosion Science, 2009, 51: 690−698.

[36] MCCAFFERTY E. Introduction to corrosion science [M]. New York: Springer, 2010.

[37] ZHANG Xiao-ge. Gregory. Corrosion and electrochemistry of zinc [M]. New York: Plenum Press, 1996.

[38] EL-FEKI A, WALTER G W. Corrosion rate measurements under conditions of mixed charge transfer plus diffusion control including the cathodic metal ion deposition partial reaction [J]. Corrosion Science, 2000, 42: 1055−1070.

[39] HASSAN H H. Perchlorate and oxygen reduction during Zn corrosion in a neutral medium [J]. Electrochimica Acta, 2006, 51: 5966−5972.

氯化钠溶液中腐蚀对复合铸造 ZA27/SiC_p 复合材料表观和显微组织的影响

Biljana BOBIĆ[1], Jelena BAJAT[2], Ilija BOBIĆ[3], Bore JEGDIĆ[1]

1. Institute of Chemistry, Technology and Metallurgy, University of Belgrade, Belgrade 11000, Serbia;
2. Faculty of Technology and Metallurgy, University of Belgrade, Belgrade 11000, Serbia;
3. "Vinča" Institute of Nuclear Sciences, University of Belgrade, Belgrade 11000, Serbia

摘　要：ZA27/SiC_p 复合材料在氯化钠溶液中浸泡 30 d，通入氧气，研究腐蚀对其表观和显微组织的影响。通过复合铸造制备不同 SiC 粒子含量的复合材料。采用光学显微镜和扫描电子显微镜研究材料的显微组织，结果表明复合材料基体发生了腐蚀，且优先发生在富锌 η 相。腐蚀过程不影响嵌入基体合金中的 SiC 粒子。电化学极化测试表明，复合材料中 SiC 粒子含量的增加，导致复合材料的耐腐蚀性降低。

关键词：金属基复合材料；ZA27 合金；腐蚀；显微组织；极化电阻；腐蚀率

(Edited by Xiang-qun LI)